$\langle A^2 \rangle$ asymmetry in lattice $SU(2)$ gluodynamics at $T > T_c$

V. G. Bornyakov

Institute for High Energy Physics, NRC "Kurchatov Institute", 142281 Protvino, Russia, School of Biomedicine, Far East Federal University, 690950 Vladivostok, Russia, and Institute of Theoretical and Experimental Physics, NRC "Kurchatov Institute", 117259 Moscow, Russia

V. K. Mitrjushkin

Joint Institute for Nuclear Research, 141980 Dubna, Russia

R. N. Rogalyov

Institute for High Energy Physics, NRC "Kurchatov Institute", 142281 Protvino, Russia

(Received 7 October 2016; revised manuscript received 21 May 2019; published 21 November 2019)

We study numerically the chromoelectric-chromomagnetic asymmetry of the dimension two A^2 gluon condensate at $T > T_c$ in the Landau-gauge $SU(2)$ lattice gauge theory with a particular emphasis on finite-volume effects. We show that previously found so called symmetric point at which asymmetry changes sign is an artifact of the finite volume effects. We find that with increasing temperature the asymmetry decreases approaching zero value from above in agreement with the perturbative result.

DOI: 10.1103/PhysRevD.100.094505

I. INTRODUCTION

Studies of the dimension-two gauge-boson condensate

$$\langle A^2 \rangle = g^2 \sum_{\mu=1}^{4} \sum_{a=1}^{3} \langle A_\mu^a(x) A_\mu^a(x) \rangle \tag{1}$$

in the last 15 years were initiated by Ref. [1], where it was shown that the nonperturbative part of $\langle A^2 \rangle$ is completely determined by contribution of the topological defects (monopoles) responsible for confinement in the compact electrodynamics. Since monopole condensation is one of the most popular scenarios of confinement also in non-Abelian gauge theories, this observation suggested that the gluon dimension-two condensate plays an important role in the studies of infrared properties of Yang–Mills theories as well.

In spite of some earlier considerations of the composite operator $A^2(x) = \sum_{\mu=1}^{4} \sum_{a=1}^{3} A_\mu^a(x) A_\mu^a(x)$ ([2], etc.), for long time it was disregarded in the operator product expansion (OPE) approach because of its gauge dependence.

In the Landau gauge, the operator $A^2(x)$ is BRST invariant (on mass shell) and multiplicatively renormalizable, as was shown in [3,4] in the $\overline{\text{MS}}$ scheme. Later it was argued [5] that the matrix element $\langle A^2 \rangle$ is gauge-invariant in spite of gauge dependence of the respective operator, still it does not appear in the expansions of products of gauge-invariant composite operators [6].

The effective potential for $\langle A^2 \rangle$ was obtained in [3,7] indicating nonvanishing value of $\langle A^2 \rangle$ and thus dynamical gluon mass generation.

In the OPE approach, $\langle A^2 \rangle$ was used for the parametrization of soft nonperturbative contributions to the Green functions, for a review see [8]. Thus it was extracted from their high momentum behavior [9,10].

It was shown that, over the momentum range $2.5 \div 7$ GeV, ghost and gluon propagators evaluated on a lattice agree with the respective perturbative estimates only when corrections due to $\langle A^2 \rangle$ condensate are taken into account [11,12].

In a series of papers (see, e.g., [8,13] and references therein) $\langle A^2 \rangle$ was computed numerically from fits to lattice data for the gluon and ghost propagators as well as 3-gluon and ghost-gluon vertices. For example, in a specific MOM-type renormalization scheme defined by a zero incoming ghost momentum[1] ($\mu = 10$ GeV), the following values for the $N_f = 2 + 1 + 1$ QCD were found [14]:

$\langle A^2 \rangle = 2.8(8)$ GeV^2 (OPE up to $\frac{1}{p^4}$)

$\langle A^2 \rangle = 3.8(6)$ GeV^2 (OPE up to $\frac{1}{p^6}$)

in order to obtain the QCD coupling constant $\alpha_{\overline{MS}}(M_Z) = 0.1198(4)(8)(6)$.

[1]Also referred to as the Taylor scheme.

The $\langle A^2\rangle$ condensate was also intensively studied in the refined Gribov-Zwanziger (RGZ) approach [15–17]. Other studies of this condensate include [18–20].

In Ref. [1] the $\langle A^2\rangle$ was related to the confinement-deconfinement transition in $4D$ compact $U(1)$ gauge theory. In this theory the confinement and deconfinement phases are separated by the phase transition at zero temperature. It was found that the nonperturbative part of the condensate drops at critical coupling. This observation raised hopes that the $\langle A^2\rangle$ condensate might be also of relevance for the finite temperature transition in the $4D$ non-Abelian theories.

There are two A^2 condensates at nonzero temperature, electric $\langle A_E^2\rangle$, and magnetic $\langle A_M^2\rangle$:

$$\langle A_E^2\rangle = g^2\sum_{a=1}^{3}\langle A_4^a(x)A_4^a(x)\rangle,$$
$$\langle A_M^2\rangle = g^2\sum_{i=1}^{3}\sum_{a=1}^{3}\langle A_i^a(x)A_i^a(x)\rangle. \tag{2}$$

The quantity of particular interest is the (color) electric-magnetic asymmetry introduced in [21]:

$$\langle \Delta_{A^2}\rangle \equiv \langle A_E^2\rangle - \frac{1}{3}\langle A_M^2\rangle. \tag{3}$$

Later we will also use the dimensionless quantity

$$\mathcal{A} = \frac{\langle \Delta_{A^2}(x)\rangle}{T^2}. \tag{4}$$

Within the OPE approach and in the $p_4 = 0$ approximation, it was shown [22] that the asymmetry contributes to the quark propagator at nonzero temperatures.

The main interest in the asymmetry stems from its possible relation to both the confinement-deconfinement transition and dynamics in the deconfinement phase.

In [21] the asymmetry was computed for the first time in lattice $SU(2)$ gluodynamics for a wide range of temperatures in both confinement and deconfinement phases. It was found that it peaks at the phase transition and monotonically decreases with increasing temperature in the deconfinement phase. Furthermore, it was found that the asymmetry crosses zero at $T \approx 2.2T_c$ and becomes negative at higher temperatures. The existence of this symmetric point was one of the main results of Ref. [21].

In this paper we make a number of improvements in computation of the asymmetry in comparison with Ref. [21]. We take care of the finite-volume and Gribov-copy effects. As a result we demonstrate that the asymmetry is indeed monotonically decreasing function in the deconfinement phase but it never turns zero. This result is in a qualitative agreement with the perturbative calculations, see below. Thus we demonstrate that the asymmetry cannot serve as an indicator of the boundary of the postconfinement domain.

We introduce necessary notations and describe simulation details in the next section. In Sec. III we reproduce qualitatively results of Ref. [21] and demonstrate that computation of the asymmetry in [21] suffers from large finite volume effects. We also present results of our study of the Gribov copy effects in this section. Section IV is devoted to the temperature dependence of the asymmetry. Finally, we conclude in Sec. V.

II. DEFINITIONS AND SIMULATION DETAILS

We study SU(2) lattice gauge theory with the standard Wilson action

$$S = \beta\sum_x\sum_{\mu>\nu}\left[1 - \frac{1}{2}\mathrm{Tr}(U_{x\mu}U_{x+\mu;\nu}U^\dagger_{x+\nu;\mu}U^\dagger_{x\nu})\right],$$

where $\beta = 4/g^2$ and g is a bare coupling constant. The link variables $U_{x\mu} \in SU(2)$ transform under gauge transformations ω_x as follows:

$$U_{x\mu}\overset{\omega}{\mapsto}U^\omega_{x\mu} = \omega_x^\dagger U_{x\mu}\omega_{x+\mu}; \qquad \omega_x \in SU(2). \tag{5}$$

Our calculations were performed on the asymmetric lattices with lattice volume $V = N_t \times N_s^3$, where N_t is the number of sites in the $4th$ direction. The temperature T is given by

$$T = \frac{1}{aN_t}, \tag{6}$$

where a is the lattice spacing. We employ the standard definition of the lattice gauge vector potential[2] $A_{x,\mu}$ [23]:

$$A_{x,\mu} = \frac{1}{2iag}(U_{x\mu} - U^\dagger_{x\mu}) \equiv \sum_{a=1}^{3}A^a_{x,\mu}\frac{\sigma_a}{2}, \tag{7}$$

where a are color indices, σ_a are Pauli matrices.

The lattice Landau gauge fixing condition is

$$(\nabla^B A)_x \equiv \frac{1}{a}\sum_{\mu=1}^{4}(A_{x,\mu} - A_{x-a\hat{\mu},\mu}) = 0, \tag{8}$$

which is equivalent to finding an extremum of the gauge functional

[2]In perturbation theory, $A_{x+\hat{\mu}/2,\mu}$ instead of $A_{x,\mu}$ provides a more adequate designation; $\hat{\mu}$ is the unit vector in the μth direction.

$$F_U(\omega) = \frac{1}{4V}\sum_{x,\mu}\frac{1}{2}\mathrm{Tr}U^{\omega}_{x\mu}, \tag{9}$$

with respect to gauge transformations ω_x. After replacing $U \Rightarrow U^{\omega}$ at the extremum the gauge condition (8) is satisfied.

In terms of lattice variables, the asymmetry has the form

$$\mathcal{A} = \frac{4a^2N_t^2}{\beta}\sum_{b=1}^{3}\left(\langle A^b_{x,4}A^b_{x,4}\rangle - \frac{1}{3}\sum_{i=1}^{3}\langle A^b_{x,i}A^b_{x,i}\rangle\right). \tag{10}$$

It can be expressed in terms of the gluon propagators:

$$\mathcal{A} = \frac{4N_t}{\beta a^2 N_s^3}\left[3(D_L(0) - D_T(0)) + \sum_{p\neq 0}\left(\frac{3|\vec{p}|^2 - p_4^2}{p^2}D_L(p) - 2D_T(p)\right)\right] \tag{11}$$

where $D_L(D_T)$ is the longitudinal (transversal) gluon propagators. In the continuum limit, the respective integral is ultraviolet finite [21,24]; therefore, no additional renormalization is needed and this formula holds true for renormalized quantities as well. Thus the asymmetry $\mathcal{A}$, which is nothing but the vacuum expectation value of the respective composite operator, is multiplicatively renormalizable and its renormalization factor coincides with that of the propagator.[3]

The authors of [24] obtained one-loop perturbative estimates of the asymmetry both at high temperatures

$$\langle\Delta_{A^2}\rangle \simeq \frac{g^2T^2}{4}\left(1 - \frac{g}{3\pi}\sqrt{\frac{2}{3}}\right) \tag{12}$$

and at low temperatures

$$\langle\Delta_{A^2}\rangle \simeq \frac{g^2\pi^2}{10}\left(1 - \frac{85}{522}\frac{g^2}{16\pi^2}\right)\frac{T^4}{M^2}, \tag{13}$$

where

$$M^2 = -\frac{13}{54}\langle A^2(T=0)\rangle.$$

We have generated ensembles of $O(1500)$ independent Monte Carlo lattice field configurations. Consecutive configurations (considered as independent) were separated by $100 \div 200$ (for $N_s = 24 \div 88$) sweeps, each sweep consisting of one local heatbath update followed by $N_s/2$ microcanonical updates. In Appendix A, we provide information about the ensembles used throughout this paper.

In the gauge fixing procedure we employ the $Z(2)$ transformation proposed in [25]. $Z(2)$ flip in direction μ consists in flipping all link variables $U_{x\mu}$ attached and orthogonal to a 3d plane by multiplying them with -1. Such global flips are equivalent to nonperiodic gauge transformations and represent an exact symmetry of the pure gauge action. The Polyakov loops in the direction of the chosen links and averaged over the 3d plane obviously change their sign. At finite temperature we apply flips only to directions $\mu = 1, 2, 3$, thus we consider 8 flip sectors. In the deconfinement phase, where the $Z(2)$ symmetry is broken, the $Z(2)$ sector of the Polyakov loop in the $\mu = 4$ direction has to be chosen since on large enough volumes all lattice configurations belong to the same sector, i.e., there are no flips between sectors in the Markov chain of configurations. We choose the sector with positive Polyakov loop. We begin simulations with the cold start and at the temperature values and lattice sizes studied in this paper we did not observe the flips to the negative Polyakov loop sector with only one exception.[4]

Following Ref. [26] in what follows we call the combined gauge fixing algorithm employing simulated annealing (SA) algorithm (with finalizing overrelaxation) and $Z(2)$ flips for space directions the "FSA" algorithm. We generated $n_{\mathrm{copy}} = 2$ gauge copies per flip-sector each time starting from a random gauge transformation of the Monte Carlo configuration, obtaining in this way $N_{\mathrm{copy}} = 8 \cdot n_{\mathrm{copy}}$ Landau-gauge fixed copies for every configuration. We take the copy with maximal value of the functional (9) as our best estimator of the global maximum and denote it as best ("bc") copy. In order to demonstrate the Gribov copy effect we compare with the results obtained from the randomly chosen first ("fc") copy and with the "worst" copy ("wc"), i.e., copy with the lowest value of the gauge functional [27]. The worst copy results are to demonstrate that the Gribov copy effects within first Gribov horizon are substantially stronger than the difference between our first copy and best copy.

III. FINITE VOLUME AND GRIBOV COPY EFFECTS

The asymmetry was introduced and studied numerically in [21] in a rather wide range of temperatures ($0.4T_c < T < 6T_c$). The computations were made on the lattices $16^3 \times 4$, $24^3 \times 6$, and $32^3 \times 8$. A nontrivial temperature dependence was obtained. In particular, it was found that the asymmetry is positive at $T < 2.21(5)T_c$ and negative at $T > 2.21(5)T_c$. This observation was

[3]We assume that $D_L(p)$ and $D_T(p)$ are renormalized with the same factor.

[4]The flip happened on the $28^3 \times 8$ lattice corresponding to lattice size 2 fm and $T = 1.16T_c$. For this lattice we discarded configurations with negative Polyakov loop.

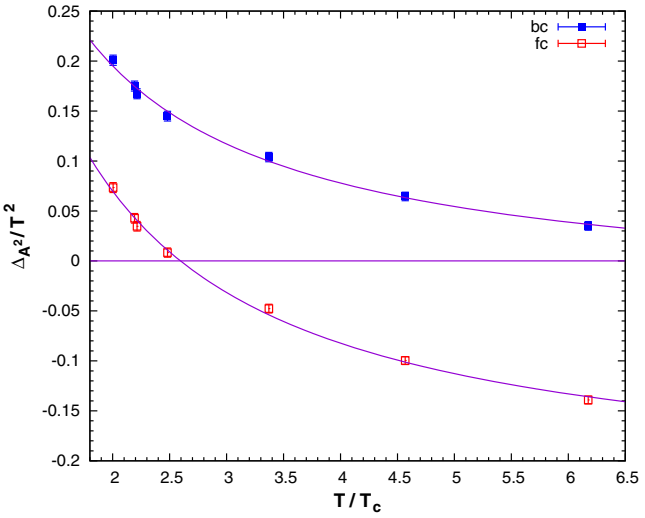

FIG. 1. Asymmetry on lattices $32^3 \times 8$ as function of temperature. Lower dataset shows our results for first copy and should be compared with that obtained in [21]. Upper dataset was obtained with the FSA algorithm (best copy). The curves show results of the fits to Eq. (17).

considered as an indication that at high temperatures magnetic fluctuations begin to dominate. Comparing data for three lattice spacings the authors concluded that finite lattice spacing effects are small even for $N_t = 4$. This allows us to assume that our results obtained on lattices with $N_t = 8$ are also free of substantial finite lattice spacing effects.

Let us note that in [21] (as well as in this work) the temperature was changed by variation of the lattice spacing for fixed N_t. In Ref. [21] the finite volume effects were not checked although the spatial lattice size was decreasing with increasing temperature and at the highest temperature $T = 6T_c$ it was as small as $L \equiv aN_s = 0.44$ fm with the corresponding minimal momentum $p_{\min} \simeq 2.8$ GeV. In this work we carefully study the finite volume effects using lattices up to $L \approx 5$ fm (the detailed information on lattices used in this work is given in Appendix A). Furthermore, we use Z_2 flips which help to reduce finite volume effects as was found in Ref. [28]. Here we again show that the effect of flip sectors is very substantial on small volumes. We then demonstrate that taking care about the finite volume effects dramatically changes some of the conclusions made in [21].

First, we want to show that our first copy results reproduce qualitatively well the results obtained in [21] at high temperatures ($2 \lesssim T/T_c \lesssim 6$).

In Fig. 1 we show our results for $\mathcal{A}$ obtained on lattices $32^3 \times 8$ used in [21]. The lower data set shows our results for the first copy (fc). These results are to be compared with those obtained in [21]. The upper data set corresponds to the best copy (bc). One can see that two data sets differ dramatically and this difference grows with temperature.

To make explicit comparison with [21], we fit data points corresponding to fc copy to the function

$$\mathcal{A} = b_0 + \frac{b_2}{\xi^2}, \tag{14}$$

used in [21]; here and below $\xi = T/T_c$. This function does not fit our data well, $\chi^2/N_{\rm dof} = 8.1$, but the parameters obtained in our fit,

$$b_0 = -0.15(1), \qquad b_2 = [0.959(31)]^2, \tag{15}$$

agree qualitatively well with those found in [21]:

$$b_0 = -0.164(4), \qquad b_2 = [0.894(14)]^2. \tag{16}$$

Our value $\xi = 2.50(22)$ at which $\mathcal{A}_{fc} = 0$ is only a little higher than the respective value $\xi = 2.21(5)$ from [21]. We conclude that our values of $\mathcal{A}_{fc}$ come close to the values of the asymmetry obtained in [21].

Now we turn to the upper data set. It differs significantly from both the fc data set and the results of [21]. The main qualitative difference is that $\mathcal{A}_{bc}$ does not cross zero within the range of temperatures under study. Since the difference between the two procedures employed to obtain these two data sets consists in the use of flips, we attribute the observed difference to the flip effects. As was shown in [28] the use of flips substantially reduces finite volume effects, thus we expect that the observed difference increases with a decrease of the lattice size.

For both bc and fc data sets we find that our data for $N_s = 32$ are much better fitted by the fit function

$$\mathcal{A} \simeq b_0 + \frac{b_1}{\xi}. \tag{17}$$

For the bc data, the fit parameters are

$$b_0 = -0.039(5), \qquad b_1 = 0.469(14), \tag{18}$$

and $\chi^2/N_{\rm dof} = 0.91$, whereas the alternative fit function (14) gives $\chi^2/N_{\rm dof} = 3.53$ and thus should be disregarded. We conclude that even if $\mathcal{A}_{bc}$ at $N_s = 32$ becomes negative, this occurs at temperatures much greater than the upper limit of the range under our consideration.

Next we proceed to the study of the finite-volume dependence of the asymmetry and infinite volume extrapolation at two values of temperature. In Fig. 2 we show lattice-size dependence of the asymmetry at $T/T_c = 1.49$ (filled symbols) and $T/T_c = 2.49$ (empty symbols). As is seen in Fig. 2, the volume dependence of $\mathcal{A}_{fc}$ is very significant (in the wc case situation is much worse) and $\mathcal{A}_{fc}$ even changes sign at $L \simeq 1.3$ fm for $T/T_c = 1.49$ and at $L \simeq 1.0$ fm for $T/T_c = 2.49$. As expected the finite-size effects for bc are much smaller than for fc and this is due to flips. Our data indicate that to reduce the finite-size effects below, say, 3% one needs the lattice size $L \gtrsim 2.5$ fm in the bc case, $L \gtrsim 4$ fm in the fc case, and $L \gtrsim 5$ fm in the wc

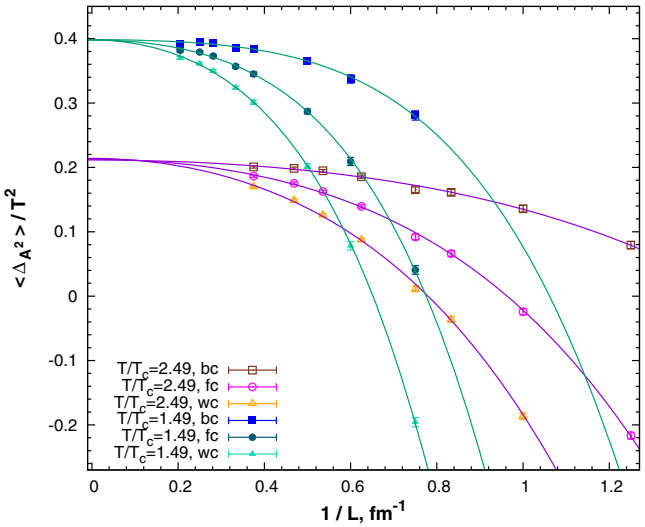

FIG. 2. Lattice size dependence of the asymmetry at $T/T_c = 1.49$ (filled symbols) and 2.49 (empty symbols). Results are presented for bc (squares), fc (circles), and wc (triangles). Curves show results of the fit to Eq. (20).

case. This holds true for both $T/T_c = 1.49$ and $T/T_c = 2.49$. To extrapolate the asymmetry to the infinite volume limit $\mathcal{A}_\infty$ we begin with the polynomial fit of the type[5]

$$\mathcal{A}(L) = \mathcal{A}_\infty^{\mathrm{pol}} - \frac{c_2}{L^2} - \frac{c_4}{L^4}, \tag{19}$$

the results are shown in Table I.

To estimate systematic errors due to choice of the fitting function, we also fitted the data to the following fit functions with the same number of the fit parameters:

$$\mathcal{A}(L) \simeq \mathcal{A}_\infty^{\mathrm{exp}} - c\exp(-L/L_0) \tag{20}$$

and

$$\mathcal{A}(L) \simeq \mathcal{A}_\infty^{\mathrm{pow}} - c^b/L^b. \tag{21}$$

The results of these fits are presented in Appendix B. One can see that the function (20) provides a good fit for bc results only, while the function (21) fits both data sets well. In all cases when the fit is good we find the values of $\mathcal{A}_\infty^{\mathrm{pol}}$, $\mathcal{A}_\infty^{\mathrm{exp}}$, and $\mathcal{A}_\infty^{\mathrm{pow}}$ to agree within 2σ. This implies that the systematic error is of the same order as the statistical one.

[5]We found that the fit function $\mathcal{A}(L) = \mathcal{A}_\infty^{\mathrm{pol}} - \frac{c_1}{L} - \frac{c_2}{L^2}$ can also produce good fits. It was discarded since it predicts for asymmetry a change of decreasing to increasing with increasing $1/L$ at $1/L \approx 0.2$ fm^{-1}, thus introducing an unexpected scale of the order of 5 fm. Moreover, data obtained on even larger lattices ($L \sim 8$ fm, $N_t = 4$, not presented in this paper) rule out this fit function whereas the fit functions considered here provide good fits for these large lattices too.

TABLE I. Results of fitting of the asymmetry to polynomial fit Eq. (19).

ξ	Gauge fixing algorithm	$\mathcal{A}_\infty^{\mathrm{pol}}$	$\sqrt{c_2}$, fm	$\sqrt[4]{c_4}$, fm	$\frac{\chi^2}{N_{\mathrm{dof}}}$
1.49	bc	0.3983(32)	0.26(6)	0.71(4)	0.80
1.49	fc	0.3976(22)	0.54(3)	0.89(2)	0.74
2.49	bc	0.2114(26)	0.248(22)	0.35(4)	0.98
2.49	fc	0.2127(29)	0.402(15)	0.52(1)	1.26

Another observation following from Fig. 2 is that for all three gauge fixing procedures (bc, fc, and wc) values for the asymmetry agree well in the infinite volume limit. This is in agreement with our results for the gluon propagator obtained in $3D$ $SU(2)$ gluodynamics [27]. This result implies that effect of the Z_2 flips used in our gauge fixing procedure to obtain bc copies disappears in the infinite volume limit while effects of two copies generated for every Z_2 sector are small on our volumes. These implications will be confirmed later in this section.

To study the Gribov copy effects quantitatively we compute the following relative deviation [29]:

$$D_{\mathrm{GCE}} = \frac{\mathcal{A}_{bc} - \mathcal{A}_{fc}}{\mathcal{A}_{bc}}. \tag{22}$$

To consider the effects of Z_2 flips and effects of Gribov copies within a flip sector separately we also introduce

$$D_{\mathrm{flip}} = \frac{\mathcal{A}_{bc1} - \mathcal{A}_{fc}}{\mathcal{A}_{bc1}}, \tag{23}$$

and

$$D_{\mathrm{SE}} = \frac{\mathcal{A}_{bc} - \mathcal{A}_{bc1}}{\mathcal{A}_{bc}}, \tag{24}$$

where $\mathcal{A}_{fc}$ is asymmetry for the first copy and $\mathcal{A}_{bc1}$ is asymmetry for the best copy obtained with $n_{\mathrm{copy}} = 1$. In the case when we do not consider Z_2 sectors (as is usually done by other authors) $D_{\mathrm{GCE}} = D_{\mathrm{SE}}$. If, in opposite, we take $n_{\mathrm{copy}} = 1$ then $D_{\mathrm{GCE}} = D_{\mathrm{flip}}$. In the general case the three quantities satisfy the following relation:

$$D_{\mathrm{GCE}} = D_{\mathrm{flip}} + D_{\mathrm{SE}} - D_{\mathrm{flip}} \cdot D_{\mathrm{SE}}. \tag{25}$$

This relation simplifies when both D_{flip} and D_{SE} are small. Then one can discard the last term to arrive at

$$D_{\mathrm{GCE}} \approx D_{\mathrm{flip}} + D_{\mathrm{SE}}. \tag{26}$$

Our data indicate that D_{SE} decreases with volume and for lattice size $L > 1$ fm it is substantially smaller than D_{flip}: for $L > 1$ fm and $T/T_c \in \{1.49, 2.49\}$ $\frac{D_{\mathrm{SE}}}{D_{\mathrm{flip}}} < \frac{1}{6}$. For this reason in what follows we use the approximation $D_{\mathrm{GCE}} \approx D_{\mathrm{flip}}$.

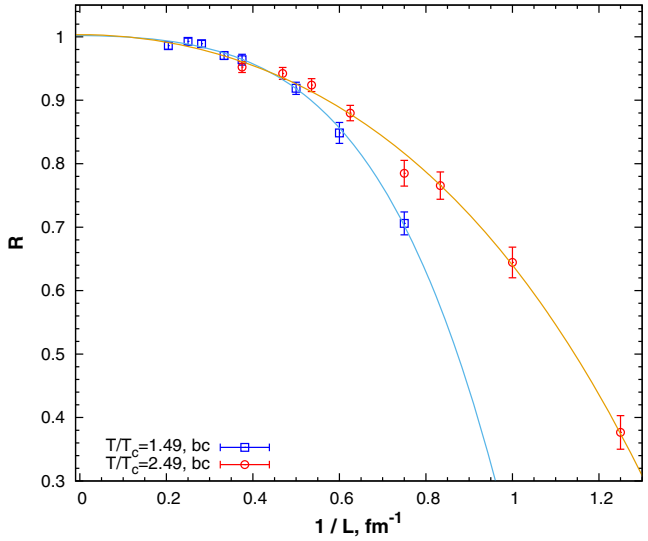

FIG. 3. bc results for the asymmetry normalized by its infinite volume value to compare finite volume effects at two temperatures, $T/T_c = 1.49$ and 2.49. Curves show results of the fit to Eq. (20).

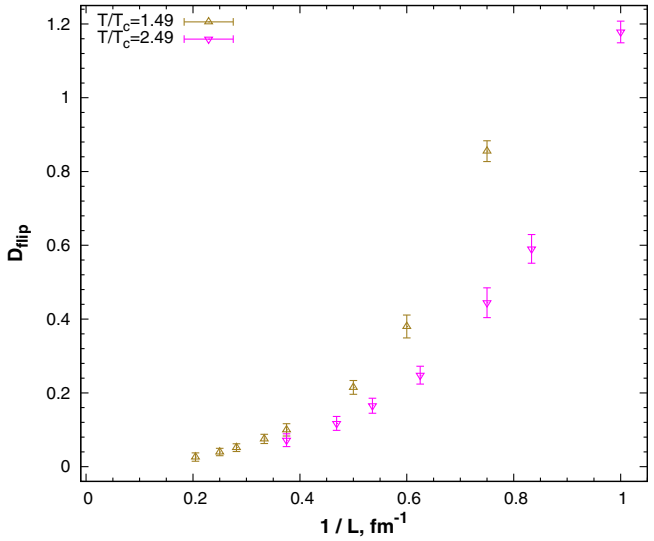

FIG. 4. Relative deviation D_{flip} for asymmetry, see Eq. (23) for definition. It demonstrates flip effects dependence on lattice size and temperature.

It should be mentioned that the dependence of the asymmetry on n_{copy} on large lattices is still to be investigated. Thus we cannot exclude that D_{GCE} is nonzero in the infinite volume limit despite the equality between the bc and fc results in this limit demonstrated in Fig. 2.

It is known that at high temperature the $SU(2)$ gluodynamics undergoes dimensional reduction and the correlation lengths decrease with increasing temperature as $1/gT$ or $1/g^2T$. This implies that for a fixed physical lattice size L the finite volume effects should decrease with increasing temperature. To observe this decreasing in our data we plot in Fig. 3 the $\mathcal{A}$ values (only for bc copies) normalized by the respective infinite volume limits:

$$R = \mathcal{A}/\mathcal{A}_\infty. \tag{27}$$

One can see clearly decreasing of the finite volume effects for $T/T_c = 2.49$ in comparison with $T/T_c = 1.49$ when $L \lesssim 2$ fm. For lattice size $L \gtrsim 2$ fm the finite volume effects for both temperatures are of the same size within statistical errors and are below 8%. We thus consider physical lattice size $L \gtrsim 2$ fm as sufficient to avoid large finite volume effects in the temperature range studied in this paper. In the next section we will use this observation in our study of the temperature dependence.

We depict in Fig. 4 the relative deviation D_{flip}. One can see that effect of the flips goes to zero in the infinite volume limit for both temperatures shown in the figure. Another observation is that similarly to the finite volume effects flip effects decrease with increasing temperature for lattice size up to $L \lesssim 2.5$ fm, and show temperature independence (within our numerical precision) for $L \gtrsim 2.5$ fm.

We checked finite size effects for the dimension two electric $\langle A_E^2 \rangle$ and magnetic $\langle A_M^2 \rangle$ condensates separately. We found that the electric condensate is constant within error bars, whereas the magnetic one decreases with increasing volume. Thus the finite size effects found in the asymmetry are due to volume dependence of the magnetic condensate.

IV. TEMPERATURE DEPENDENCE

In this section we consider the temperature dependence of the condensate. The results were obtained for the fixed lattice size $L = 2$ fm in the temperature range $1.2 < \xi < 3.5$ as well as for $L = 3$ fm for reduced temperature range $1.2 < \xi < 2.5$

The results for bc, fc and wc on lattices with $L = 2$ fm and varying temperature are shown in Fig. 5. We checked that a good fit is provided by the function (14) for all three data sets for $\xi > 1.6$. The respective fit parameters are shown in Table II. It occurred that for $L = 3$ fm the fit (14) does not work in our range of temperatures ($\chi^2/N_{\text{dof}} = 5.13$ for the range $1.5 < T/T_c < 2.5$).

Still, for both lattice sizes our results indicate that the asymmetry is positive at all temperatures. This is in agreement with the perturbative result (12). The expression (14) disagrees with the perturbative result (12) in the limit of infinite temperature where perturbation theory is believed to be valid. For this reason, we find it useful to fit the data to the function [motivated by (12)]

$$\mathcal{A} \simeq \frac{z g^2(T)}{4}\left(1 - \frac{g(T)}{3\pi}\sqrt{\frac{2}{3}}\right), \tag{28}$$

where the running coupling is taken in the two-loop approximation [30],

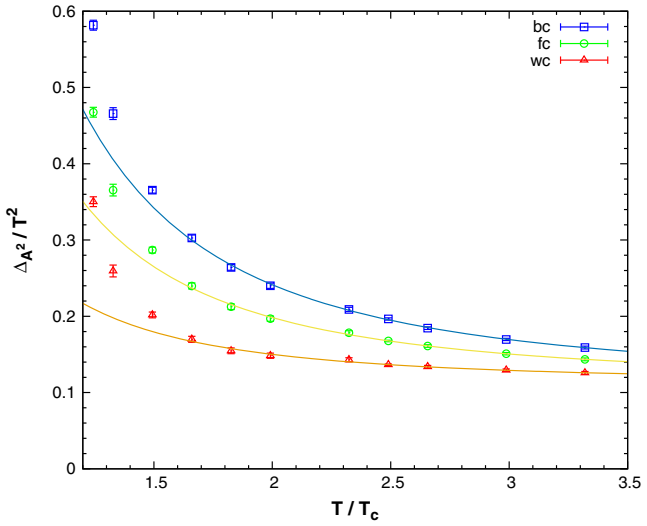

FIG. 5. Asymmetry as function of the temperature for the fixed lattice size $L = 2$ fm. The curves show the fit function (14) for $\xi > 1.6$.

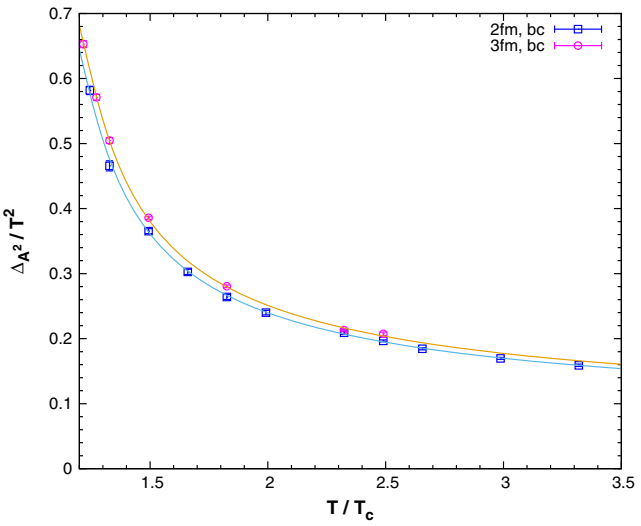

FIG. 6. $\mathcal{A}$ for bc for both $L = 2$ fm and $L = 3$ fm. Curves show fits to the function (28).

$$\frac{1}{g^2(T)} = \frac{1}{4\pi^2}\left(\frac{11}{6}\ln\left(\frac{T^2}{\Lambda^2}\right) + \frac{17}{11}\ln\ln\left(\frac{T^2}{\Lambda^2}\right)\right), \qquad (29)$$

z and Λ are the fit parameters.

The results of the fits for $\xi > 1.2$ for the two lattice sizes are shown in Table III and depicted in Fig. 6. Note that this fit works much better (smaller $\chi^2/N_{\rm dof}$ and/or wider range of applicability) than the fit (14). In particular, the fit (14) has very large $\chi^2/N_{\rm dof}$ (29 and 57 for $L = 2$ fm and 3 fm, respectively) for the range $\xi > 1.2$ used for fit (28). Therefore, we arrive at a good agreement with perturbation theory modulo the normalization factor of the propagator. Similar agreement with perturbative behavior was found for a screening mass, e.g., in Ref. [30]. In order to make quantitative comparison with the perturbative result, we should use the same normalization condition; however, the $\overline{\rm MS}$ scheme employed in [24] runs into difficulties beyond perturbation theory.

TABLE II. Parameters of the fit of the asymmetry to Eq. (14). Lattice size 2 fm, $\frac{T}{T_c} > 1.6$.

Gauge fixing algorithm	b_0	b_2	$\frac{\chi^2}{N_{\rm dof}}$
bc	0.112(2)	0.518(11)	0.71
fc	0.113(2)	0.344(11)	0.78
wc	0.113(2)	0.151(12)	0.92

TABLE III. Parameters of the fit of the asymmetry to Eq. (28).

L	z	Λ/T_c	$\frac{\chi^2}{N_{\rm dof}}$ $\xi > 1.24$
2 fm	0.1356(6)	0.8331(27)	0.56
3 fm	0.1410(13)	0.8388(35)	1.30

One can see in Fig. 6 that the difference between results for the two lattice sizes decreases with increasing temperature and the results coincide within error bars for $\xi > 2.3$ in agreement with our findings that the finite volume effects decrease with increasing temperature.

We compare temperature dependence of the asymmetry on $L = 3$ fm lattices for three gauge fixing procedures in Fig. 7. We find that the Gribov copy effect measured by $D_{\rm GCE}$ does not change throughout the range of temperatures under study, in agreement with our findings presented in the previous section (see Fig. 4). Numerically $D_{\rm GCE} \approx D_{\rm flip} \gtrsim 0.05$. Note that the respective finite-volume effects are estimated as $1 - R \leq 0.03$ (see Fig. 3).

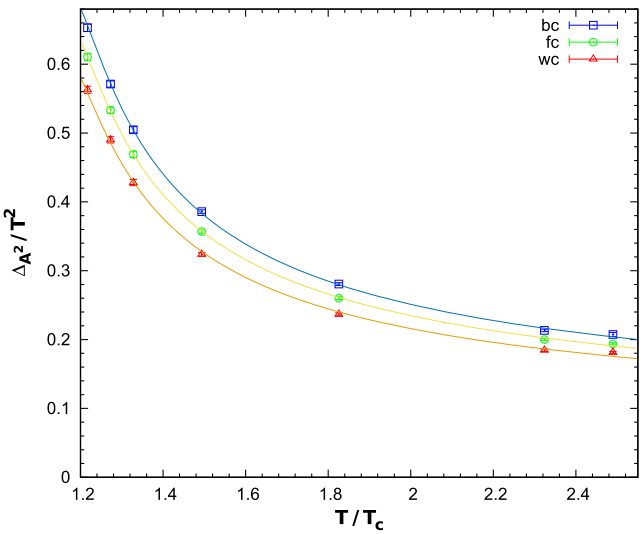

FIG. 7. $\mathcal{A}$ for all gauge-fixing procedures at $L = 3$ fm. Curves show fits to the function (28).

In contrast, for lattice size $L = 2$ fm D_{GCE} decreases substantially with increasing temperature: from about 0.2 to about 0.1. This is again in agreement with the results presented in Fig. 4. Analogous quantity introduced for wc decreases from about 0.5 to about 0.2.

Thus we infer that, contrary to the conclusions of Ref. [21], the asymmetry never crosses zero in the deconfining phase. Accordingly it cannot indicate the boundary between two regions of the deconfining phase, whose existence was discussed in [31–35].

V. CONCLUSIONS

We have presented the results of our study of the asymmetry $\mathcal{A}$ in lattice $SU(2)$ gluodynamics on lattices with varying spatial size N_s and fixed $N_t = 8$ in the range of temperatures above T_c up to $3.3T_c$. Our findings can be summarized as follows:

(i) In contrast to the conclusions made in [21], the asymmetry is positive at all temperatures under consideration and its high-temperature behavior qualitatively agrees with perturbation theory. The data can be fitted to the function (28) motivated by perturbation theory down to temperatures as low as $1.24T_c$, see Figs. 6 and 7. The asymmetry thus cannot be used as an indicator of the postconfinement domain boundary.

(ii) The fallacy in the conclusions made in [21] stems from using inadequately small lattices in that study. For this reason we have performed a careful study of finite volume effects at temperatures $T/T_c = 1.49$ and 2.49. It was demonstrated that these effects are indeed strong, see Figs. 2 and 3. Our results presented in Fig. 2 indicate that, for our best copy, the finite volume effects decrease with temperature for lattice size $L \lesssim 2$ fm and show temperature independence (within numerical precision) for bigger lattices. For our best copy the finite volume effects are below 3% on lattices with $L \gtrsim 2.5$ fm in the range of temperatures $\xi > 1.5$. Finite volume effects are much more dangerous for fc and wc gauge fixing procedures, i.e., without use of Z_2 flips. For example, to decrease them below 3% for fc one needs $L > 5$ fm.

(iii) The effect of Z_2 flips (which we consider as a part of Gribov copy effect) was estimated separately. We found that it decreases to zero in the infinite volume limit, as is shown in Fig. 4, in agreement with earlier findings for the gluon propagator. Nevertheless it is very substantial for finite volumes usually used in computations. Thus the use of flips in the study of the asymmetry is very effective. The temperature dependence of the flip effect is similar to that of the finite volume effects: for $L \lesssim 2.5$ fm they decrease with temperature and we have not observed a temperature dependence for bigger lattices.

ACKNOWLEDGMENTS

Computer simulations were performed on the IHEP (Protvino) Central Linux Cluster, ITEP (Moscow) Linux Cluster, MSU "Lomonosov" supercomputer. The work was supported by the Russian Foundation for Basic Research, Grant No. 18-02-40130.

APPENDIX A: TABLE OF STATISTICS

TABLE IV. Values of β, lattice sizes, temperatures, number of measurements, and number of gauge copies used throughout this paper. To fix the scale we take $\sqrt{\sigma} = 440$ MeV.

β	N_s	L (fm)	a^{-1} (GeV)	T (MeV)	T/T_c	n_{copy}	n_{meas}
2.5574	28	2.00	2.7622	345.3	1.162	2	3240
2.5792	30	2.00	2.9595	369.4	1.245	2	3235
2.5996	32	2.00	3.1568	394.6	1.328	2	1530
2.6706	40	2.00	3.9460	493.3	1.660	2	2160
2.7011	44	2.00	4.3406	542.6	1.826	2	1584
2.7290	48	2.00	4.7352	591.9	1.992	2	1350
2.7788	56	2.00	5.5244	690.6	2.324	2	1209
2.8221	64	2.00	6.3136	789.2	2.656	2	2064
2.8604	72	2.00	7.1028	887.9	2.987	2	1740
2.8949	80	2.00	7.8920	986.5	3.319	2	810
2.8011	24	0.80	5.919	739.9	2.490	2	3924
2.8011	30	1.00	5.919	739.9	2.490	2	2408
2.8011	36	1.20	5.919	739.9	2.490	2	1620
2.8011	40	1.33	5.919	739.9	2.490	2	1410
2.8011	48	1.60	5.919	739.9	2.490	2	2139
2.8011	56	1.87	5.919	739.9	2.490	2	2072
2.8011	64	2.13	5.919	739.9	2.490	2	1805
2.8011	80	2.67	5.919	739.9	2.490	2	1050
2.7310	32	1.33	4.764	595.5	2.00	2	2136
2.7600	32	1.21	5.213	651.6	2.19	2	2160
2.7630	32	1.20	5.261	657.6	2.21	2	2160
2.8000	32	1.07	5.899	773.4	2.48	2	2160
2.9000	32	0.79	8.016	1002	3.37	2	2136
3.0000	32	0.58	10.86	1357	4.57	2	2136
3.1000	32	0.43	14.68	1835	6.17	2	1980
2.5421	40	3.00	2.6307	328.8	1.106	2	1980
2.5574	42	3.00	2.7622	345.3	1.162	2	1566
2.5721	44	3.00	2.8937	361.7	1.106	2	1620
2.5861	46	3.00	3.0253	378.2	1.106	2	1620
2.5996	48	3.00	3.1568	394.6	1.328	2	1335
2.7011	66	3.00	4.3406	542.6	1.826	2	1760
2.7788	84	3.00	5.5244	690.6	2.324	2	886
2.6370	24	1.33	3.5514	443.9	1.494	2	3520
2.6370	30	1.67	3.5514	443.9	1.494	2	2014
2.6370	36	2.00	3.5514	443.9	1.494	2	3570
2.6370	48	1.67	3.5514	443.9	1.494	2	2096
2.6370	54	3.00	3.5514	443.9	1.494	2	2643
2.6370	64	3.56	3.5514	443.9	1.494	2	1950
2.6370	72	4.00	3.5514	443.9	1.494	2	1626
2.6370	88	4.89	3.5514	443.9	1.494	3	647

APPENDIX B: FIT RESULTS

TABLE V. Results of fitting of the asymmetry to the exponential fit Eq. (20).

ξ	Gauge fixing algorithm	$\mathcal{A}_\infty^{\exp}$	c	L_0 (fm)	$\frac{\chi^2}{N_{\mathrm{dof}}}$
1.49	bc	0.3934(12)	1.48(39)	1.95(18)	0.81
1.49	fc	0.3794(27)	3.72(64)	1.82(11)	3.74
2.49	bc	0.2019(15)	0.92(15)	2.55(18)	0.80
2.49	fc	0.1848(34)	3.77(49)	2.83(15)	5.07

TABLE VI. Results of fitting of the asymmetry to the fit Eq. (21).

ξ	Gauge fixing algorithm	$\mathcal{A}_\infty^{\mathrm{pow}}$	c	b	$\frac{\chi^2}{N_{\mathrm{dof}}}$
1.49	bc	0.3965(17)	0.68(4)	3.2(3)	0.71
1.49	fc	0.3910(16)	0.935(10)	2.96(7)	0.52
2.49	bc	0.2087(28)	0.35(3)	2.47(22)	0.87
2.49	fc	0.2032(22)	0.58(6)	2.72(6)	0.76

[1] F. V. Gubarev, L. Stodolsky, and V. I. Zakharov, Phys. Rev. Lett. **86**, 2220 (2001).
[2] M. J. Lavelle and M. Schaden, Phys. Lett. B **208**, 297 (1988).
[3] H. Verschelde, K. Knecht, K. Van Acoleyen, and M. Vanderkelen, Phys. Lett. B **516**, 307 (2001).
[4] D. Dudal, H. Verschelde, V. E. R. Lemes, M. S. Sarandy, R. F. Sobreiro, S. P. Sorella, and J. A. Gracey, Phys. Lett. B **574**, 325 (2003).
[5] A. A. Slavnov, Teor. Mat. Fiz. **143**, 3 (2005) [Theor. Math. Phys. **143**, 489 (2005)].
[6] D. V. Bykov and A. A. Slavnov, Teor. Mat. Fiz. **145**, 147 (2005) [Theor. Math. Phys. **145**, 1495 (2005)].
[7] R. E. Browne and J. A. Gracey, J. High Energy Phys. 11 (2003) 029.
[8] P. Boucaud, J. P. Leroy, A. Le Yaouanc, J. Micheli, O. Pene, and J. Rodriguez-Quintero, Few Body Syst. **53**, 387 (2012).
[9] K. Petrov, B. Blossier, P. Boucaud, O. Pene, M. Brinet, F. de Soto, V. Morenas, and J. Rodriguez-Quintero, Proc. Sci., ConfinementX (**2012**) 043 [arXiv:1304.3296].
[10] P. Boucaud, M. Brinet, F. De Soto, V. Morenas, O. Pne, K. Petrov, and J. Rodrguez-Quintero, J. High Energy Phys. 04 (2014) 086.
[11] P. Boucaud, A. Le Yaouanc, J. P. Leroy, J. Micheli, O. Pene, and J. Rodriguez-Quintero, Phys. Lett. B **493**, 315 (2000).
[12] P. Boucaud, F. De Soto, J. P. Leroy, A. Le Yaouanc, J. Micheli, O. Pene, and J. Rodriguez-Quintero, Phys. Rev. D **79**, 014508 (2009).
[13] O. Pene *et al.*, *Proc. Sci.*, FACESQCD (2010) 010 [arXiv:1102.1535].
[14] B. Blossier, P. Boucaud, M. Brinet, F. De Soto, V. Morenas, O. Pene, K. Petrov, and J. Rodriguez-Quintero (ETM Collaboration), Phys. Rev. D **89**, 014507 (2014).
[15] D. Dudal, J. A. Gracey, S. P. Sorella, N. Vandersickel, and H. Verschelde, Phys. Rev. D **78**, 065047 (2008).
[16] D. Dudal, O. Oliveira, and N. Vandersickel, Phys. Rev. D **81**, 074505 (2010).
[17] A. Cucchieri, D. Dudal, T. Mendes, and N. Vandersickel, Phys. Rev. D **85**, 094513 (2012).
[18] K.-I. Kondo, Phys. Lett. B **514**, 335 (2001).
[19] D. Dudal, H. Verschelde, and S. P. Sorella, Phys. Lett. B **555**, 126 (2003).
[20] E. R. Arriola, P. O. Bowman, and W. Broniowski, Phys. Rev. D **70**, 097505 (2004).
[21] M. N. Chernodub and E. M. Ilgenfritz, Phys. Rev. D **78**, 034036 (2008).
[22] P. Chakraborty and M. G. Mustafa, Phys. Lett. B **711**, 390 (2012).
[23] J. E. Mandula and M. Ogilvie, Phys. Lett. B **185**, 127 (1987).
[24] D. Vercauteren and H. Verschelde, Phys. Rev. D **82**, 085026 (2010).
[25] I. L. Bogolubsky, G. Burgio, V. K. Mitrjushkin, and M. Müller-Preussker, Phys. Rev. D **74**, 034503 (2006).
[26] V. G. Bornyakov, V. K. Mitrjushkin, and M. Muller-Preussker, Phys. Rev. D **81**, 054503 (2010).

[27] V. Bornyakov, V. Mitrjushkin, and R. Rogalyov, Phys. Rev. D **89**, 054504 (2014).
[28] I. L. Bogolubsky, V. G. Bornyakov, G. Burgio, E. M. Ilgenfritz, M. Muller-Preussker, and V. K. Mitrjushkin, Phys. Rev. D **77**, 014504 (2008); **77**, 039902(E) (2008).
[29] V. G. Bornyakov, V. K. Mitrjushkin, and R. N. Rogalyov, Phys. Rev. D **86**, 114503 (2012).
[30] U. M. Heller, F. Karsch, and J. Rank, Phys. Rev. D **57**, 1438 (1998).
[31] J. Liao and E. Shuryak, Phys. Rev. C **75**, 054907 (2007).
[32] M. N. Chernodub and V. I. Zakharov, Phys. Rev. Lett. **98**, 082002 (2007).
[33] J. Liao and E. Shuryak, Phys. Rev. Lett. **101**, 162302 (2008).
[34] A. Dumitru, Y. Guo, Y. Hidaka, C. P. K. Altes, and R. D. Pisarski, Phys. Rev. D **83**, 034022 (2011).
[35] M. N. Chernodub and V. I. Zakharov, Phys. At. Nucl. **72**, 2136 (2009).